

Investigation on the Grindability of CSS-42L Stainless Steel

Yang Changyong^{*}, Xu Jiuhua, Fu Yucan, Ding Wenfeng, Su Honghua

College of Mechanical and Electrical Engineering, Nanjing University of Aeronautics & Astronautics,
Nanjing 210016, P. R. China

(Received 22 December 2015 ; revised 3 May 2016; accepted 5 June 2016)

Abstract: Plunge grinding experiments were carried out on CSS-42L stainless steel with the white fused alumina wheel. The grinding forces were measured with variations in accumulated material removal volume. Then the morphological features of worn grinding wheel were analyzed by optical microscopy and the grinding temperatures were measured with a thermocouple. For comparison, C45 steel was ground under the same conditions. The results indicated that the grinding forces of CSS-42L were at least twice that of C45 steel. When the accumulated removal volume overcame 375 mm³, strong adhesion was found between the abrasives and workpiece CSS-42L. Nevertheless, adhesion was hardly found after 800 mm³ workpiece C45 steel was removed. In order to enhance the machining property of CSS-42L, a brazed CBN wheel was incorporated into the grinding of CSS-42L, and the grinding forces and temperatures were found significantly decreased, whose maximum decreasing amplitude was about 70% and 80%, respectively.

Key words: CSS-42L; grinding force; temperature; adhesion

CLC number: TG580 **Document code:** A **Article ID:** 1005-1120(2016)06-0706-08

0 Introduction

Aircraft engines represent one of the most sophisticated of engineering technologies. Gears on engine shafts have to tolerate vibratory stresses, bending moments and high rotation speeds, elevated temperatures and aggressive lubrication^[1-5]. Simultaneously, excellent toughness in the core is expected to resist continuous impact. And high temperature hardness is also needed to make gears work well. To meet all these requirements, in 1990s, researchers from the United State developed CSS-42L which bears all the properties mentioned above, and appropriate heat treatment can make it perform better^[6-7]. So this kind of steel has great potential in aviation, aerospace, shipbuilding and chemical industry. As one of the most commonly used final processing methods, grinding can eliminate distortion caused by heat treatment^[8] and determine workpiece surface integrity and, consequently, work piece

functionality^[9]. In many cases, especially for aviation gear and bear, grinding shows itself to be the only economic material removal process^[10]. However, the research on the grindability of CSS-42L has received rather limited attention. Understanding its behavior in the grinding process is therefore of vital importance.

In this study, the grindability of CSS-42L was experimentally investigated during the plunge grinding with the white fused alumina (WA) wheel and the comparative experiments were conducted on C45 steel. The rules of variations in grinding force, worn wheel surface and grinding temperature were probed in detail. Furthermore, a brazed CBN wheel was employed to grind CSS-42L to improve the grinding condition.

1 Experimental Set-up

The experimental set-up was schematically illustrated in Fig. 1. Plunge surface grinding ex-

^{*}Corresponding author, E-mail address: yangchy@nuaa.edu.cn.

periments were conducted on a HZ-Y150 surface grinder. The WA grinding wheel (WA80L5V) was used in the experiments. The diameter was 150 mm and the wheel width was 16 mm. A 5% solution of water-based emulsion was used as coolant for the grinding test.

The workpiece specimens were 25 mm along the grinding direction, 5 mm wide and initially 25 mm high. The CSS-42L specimens used in this experiment were in annealed condition, and the C45 steel specimens were in tempered condition. Spectrum analyzer was used to identify the chemi-

cal component of CSS-42L, and the result was listed in Table 1. The physical and mechanical properties of the two workpiece materials were listed in Table 2.

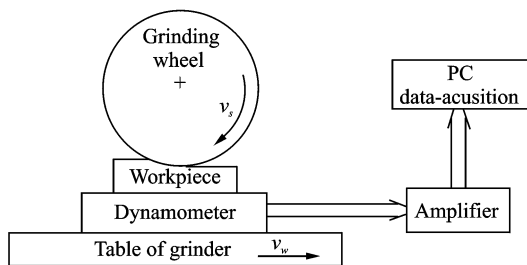


Fig. 1 Illustration of the experimental set-up

Table 1 Chemical component of CSS-42L

Element	C	Cr	V	Ni	Mo	Co	Nb	B	Mn	Si
Mass fraction/%	0.15	14.00	0.60	2.00	4.50	13.00	0.025	<0.001	<0.2	<0.25

Table 2 Physical and mechanical properties of the used workpiece materials^[7,11]

Item	CSS-42L (annealed)	C45 steel (tempered)
Density /($\text{g} \cdot \text{cm}^{-3}$)	7.93	7.85
Tensile strength (σ_b) /MPa	1 200	>600
Thermal conductivity / ($\text{W} \cdot \text{m}^{-1} \cdot \text{K}^{-1}$)	15.3	50
Hardness /HRC	35—38	28—32

The normal and tangential grinding forces, F_n and F_t , were measured using a piezoelectric transducer-based type dynamometer (Kistler 9272), coupled to charge amplifiers and a PC running Dynowear software. The sampling frequency was 3 kHz. The temperature response on the workpiece surface was measured using a grindable foil/workpiece thermocouple consisting of a constantan foil insulated on both sides by mica sheets and sandwiched between two pieces of a split workpiece. The workpiece acted as the other thermocouple pole. The cold junction was immersed in ice water. The signal was gathered by a dynamic signal recorder NI USB-6211 and analyzed in self-developed software based on Labview8.6. Smoothing and drift compensation were conducted before the grinding force signal was read so as to wipe off disturbance and guarantee the accuracy. To minimize the impact of accidents

during the test, each process was repeated at least three times, and obvious problematic data should be eliminated. The morphology of worn wheel surfaces was analyzed using a KH-7700 3D video microscope.

In the experiments, grinding wheel balancing instrument was employed to keep the wheel's balance. The WA wheel was dressed with a single-point diamond dresser to ensure a sharp tool surface.

2 Results and Analyses

Grindability of any material under industrial speed feed conditions was generally judged by various grinding responses^[12,13]. For the present study, the grinding forces and worn wheel surface were taken into consideration.

2.1 Grinding force

Grinding force is a process variable with important influence on the wheel wear, ground surface quality as well as the heat flux at the contact zone^[14, 15]. Under the condition of a wheel speed v_s of 23 m/s, a table speed v_w of 13 m/min and a depth of cut a_p of 15 μm , the normal and tangential grinding forces were measured during the continued grinding experiments, and the results were presented in Fig. 2. As can be seen from

Fig. 2, a transition period occurred during the grinding process after the truing process has been done. With 116 mm^3 workpiece having been removed, the normal grinding force of CSS-42L increased rapidly from 45 N to 115 N and the tangential grinding force increased from 30 N to 53 N. Then both of the grinding forces kept stable after the transition until the accumulated removal volume overcame 375 mm^3 . Before long both of the grinding forces fluctuated obviously. The fluctuant amplitude of the normal grinding force was 20 N and the tangential grinding force was 10 N. On the other hand, the normal grinding force of C45 steel increased to 40 N and the tangential grinding force increased to 25 N after 37.5 mm^3 C45 steel was removed. Subsequently, both of the grinding forces grew comparatively steady, and neither of the wave amplitudes exceeded 5 N. The normal grinding force of CSS-42L was more than 2.5 times that of C45 steel while the tangential force was twice that of C45 steel in plunge surface grinding with the WA wheel.

Grinding of any material may be assessed in

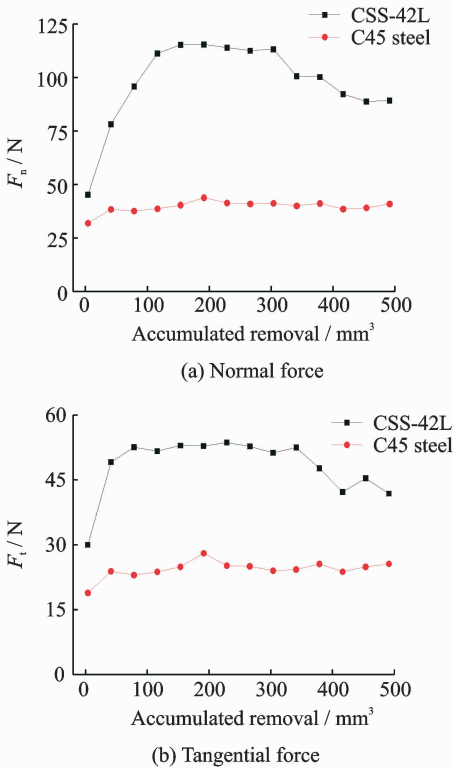


Fig. 2 Measured grinding force versus accumulated removal

terms of several responses, for example, the grinding force required, the grinding temperature and the surface integrity. However, all these responses are substantially influenced by the workpiece material characteristics. According to Table 3, the tensile strength (σ_b) of CSS-42L is about twice that of C45 steel. Compared with C45 steel, more energy was consumed when the same volume of CSS-42L was removed. Thus, the force required in the removal of CSS-42L is much more than that of C45 steel. That means, more heat was produced in the contact zone of the wheel-workpiece of CSS-42L. At the same time, the thermal conductivity of CSS-42L was only $15.3 \text{ W} \cdot \text{m}^{-1} \cdot \text{K}^{-1}$, less than one third that of C45 steel ($50 \text{ W} \cdot \text{m}^{-1} \cdot \text{K}^{-1}$). The heat evacuated by CSS-42L would be far below that of C45 steel, and consequently higher grinding temperatures would be generated quite easily in the contact zone. As a result, the WA wheel wore to dulling at a very high speed during the grinding of CSS-42L.

2.2 Morphological features of worn wheel surface

Morphological features of worn wheel surface affect the geometric accuracy and the roughness of the ground surface. Fig. 3 shows the micro-observations made on the worn surfaces of the WA wheel. It can be seen that the worn wheel surfaces, especially the chip on the surface, which underwent different accumulated removal workpiece materials, were featured with different topographies. According to previous research, chips were classified into six basic types: Flowing, shearing, ripping, knife, slice, and melting^[16], which indicate different conditions of grinding wheel. After removing 37.5 mm^3 materials, chips of CSS-42L and C45 steel were almost shearing-type and flowing-type, as shown in Figs. 3(a, b). The cutting edge of the abrasive was therefore sharp and the grinding forces were low as a result of less attritious wear of grinding wheel, as shown in Fig. 2. With the increase of the accumulated materials removal, the chips of CSS-42L became a slightly bigger, and some ad-

hered to the wheel surface, as shown in Figs. 3(c,e). After 375 mm³ workpiece material of CSS-42L were removed, the area adhering materials covered approximately 20% of the whole wheel surface, as shown in Fig. 3(g). However, obvious change of the chips of C45 steel on the

wheel surface was hardly observed until the accumulated materials removal increased up to 800 mm³. And no wheel adhesion was found on the wheel surface, as shown in Figs. 3(d,h). Also, the chips of C45 steel were constantly finer than that of CSS-42L.

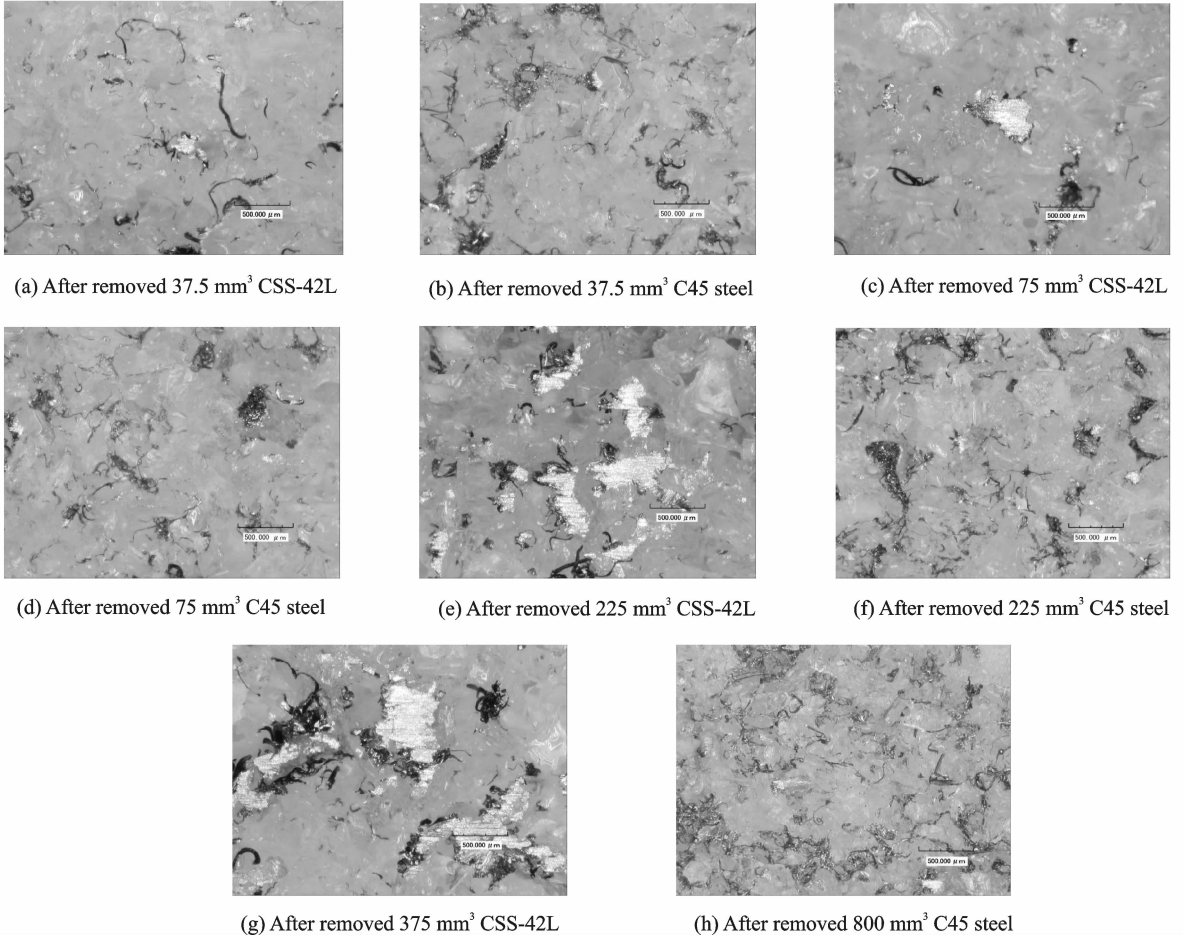


Fig. 3 Photograph for the worn surfaces of WA wheels

2.3 Grinding temperature of CSS-42L

Figs. 4, 5 show the measured grinding temperatures of CSS-42L under different experimental conditions, where v_s was 23 m/s. With the increase of table speed, the highest temperature appeared at the point of about 6 m/min and then the temperature dropped, as illustrated in Fig. 4. That would be attributed to the fact that the table speed has two "opposite" influences on the grinding temperature.

On the one hand, the increase in table speed caused the maximum undeformed chip thickness h_{\max} to grow for single grain, which can be calculated as

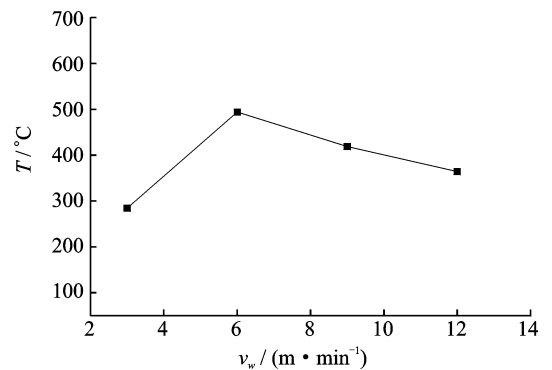


Fig. 4 Influence of table speed on grinding temperature

$$h_{\max} = \left[\frac{4v_w}{v_s N_d C} \sqrt{a_p / d_s} \right]^{1/2} \quad (1)$$

where N_d is the active cutting edge number, C a

constant and d_s , the diameter of the grinding wheel^[17].

The bigger h_{\max} meant more energy consumed, which produced more heat in the contact zone and strengthened the heat resource.

On the other hand, the heat resource moved faster and less heat was transferred into the workpiece surface with a higher table speed.

When the table speed was less than 6 m/min, the former influence served as the dominant factor in grinding CSS-42L stainless steel with WA wheels, then the grinding temperature increased with the rise in table speed. When the table speed exceeded 6 m/min, the latter influence dominated, so that an increase in table speed led directly to a drop in grinding temperature.

It can be obviously seen from Fig. 5, the temperature rose with the increasing depth of cut. The rising tendency of the curve is approximately linear. The temperature has exceeded 500 °C when the depth of cut was only about 15 μm .

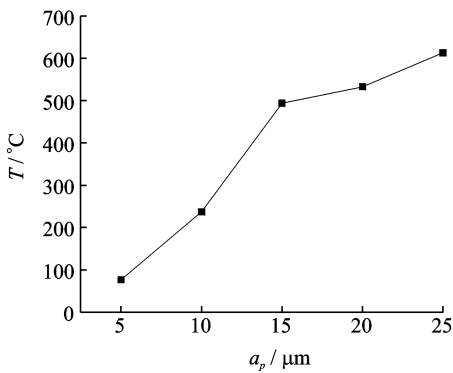


Fig. 5 Influence of depth of cut on grinding temperature

Because of the high strength and low thermal conductivity, the temperature in the contact zone between wheel and CSS-42L will be very high. The high temperature and pressure in the contact zone caused the chip of CSS-42L easier to adhere to the wheel surface, which corresponded to the photograph for the worn surfaces of WA wheels shown in Fig. 3.

3 Application of CBN Wheels

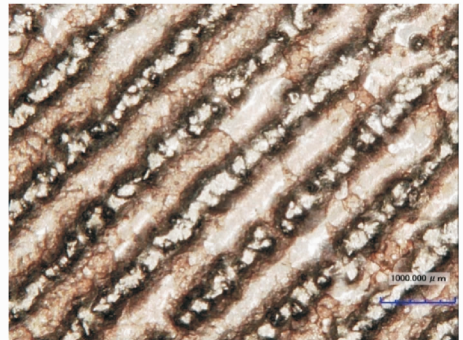
According to the above results and analyses,

the high temperature not only resulted in wheel adhesion, but also accelerated wheel wear in grinding of CSS-42L with WA wheels. Then, it is important to keep the grinding temperature low in order to achieve high performance grinding of CSS-42L. For high performance grinding, new types of CBN wheels have been developed, and experimental studies on their grinding characteristics and grinding conditions have been carried out^[18-23]. The advantage of CBN wheels have been certified in the machining of difficult-to-machine materials, such as superalloys and titanium alloys. The ground surface temperatures and grinding forces for CBN wheels are much lower than those for WA wheel with the same processing parameters. Therefore, a brazed CBN wheel was incorporated into the present study to achieve high performance grinding of CSS-42L.

The brazed CBN wheel was shown in Fig. 6, which has an external diameter of 150 mm, a working width of 9 mm and an inside diameter of 32 mm. The CBN abrasive grains were 80/100 US configured in oblique line of 45° with a spacing of 1.2 mm.



(a) Overall appearance of the wheel



(b) Configuration of grains on the surface

Fig. 6 Brazed CBN wheel

Fig. 7 displayed the variation of grinding forces of CSS-42L with the depth of cut when $v_s = 23$ m/s and $v_w = 6$ m/min. It can be obviously found that the increase of depth of cut led to the rise of both normal and tangential forces. This phenomenon was attributed to the fact that the accumulation in the depth of cut resulted in the growth in the undeformed chip thickness, as well as the length of contacting, which meant more abrasive grains took part in grinding. Therefore, the total grinding force built up. As was shown in Fig. 7, grinding forces of the brazed CBN wheel were obviously lower than those of the WA wheel for both normal and tangential forces. The largest normal and tangential forces per unit width of the CBN wheel were 2.4 N/mm and 1.4 N/mm, respectively, while for the WA wheel, they were 8 N/mm and 6 N/mm, respectively. The increase of grinding forces of CBN wheel caused by depth of cut seemed more gradual. Ground with the CBN wheel, when the depth of cut increased from 5 μm to 25 μm , the normal force rose from 0.6 N/mm to 2.4 N/mm, and the tangential force rose from 0.4 N/mm to 1.4 N/mm. But for the WA wheel, the rise seemed steep. As the depth of cut increased from 5 μm to 25 μm , the normal force grew from 1.2 N/mm to 8 N/mm, and the tangential force grew from 0.8 N/mm to 6 N/mm. This was because for the CBN wheel, abrasive grains had large outcropping height (for grains of 80/100 US, the outcropping height is about 50%–70%), which meant more storage space for chips. Besides, CBN grains have sharper blade and stronger cutting ability than

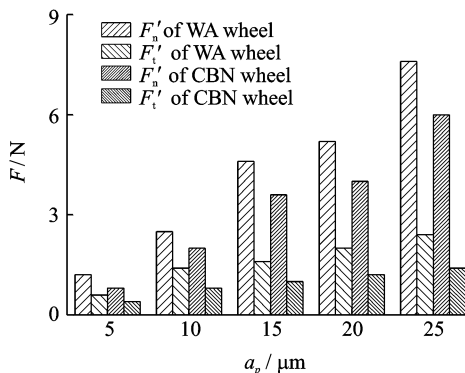


Fig. 7 Comparisons of grinding forces

WA grains, so the impact of the increase of depth of cut on the grinding force was less.

Fig. 8 shows the grinding temperatures of the two wheels with the change of the depth of cut when $v_s = 23$ m/s and $v_w = 6$ m/min. It can be easily found that the grinding temperature of the WA wheel was higher than that of the CBN wheel in all grinding parameters. For the WA wheel, the depth of cut played an important role in grinding temperature. When it was 5 μm , the grinding temperature was 80 $^{\circ}\text{C}$, and when it added to 25 μm , the grinding temperature soared to 600 $^{\circ}\text{C}$. But the situation became better when the CBN wheel was employed. As the depth of cut increased from 5 μm to 25 μm , the grinding temperature kept below 100 $^{\circ}\text{C}$ all the time, and the amplitude of variation was only 20 $^{\circ}\text{C}$ or so. The lower grinding temperature of the CBN wheel was attributed on the one hand to decrease in heat-intensity, and on the other to the high heat conductivity of the CBN abrasive grain, which is 1 300 W/(m \cdot K), almost 40 times bigger than that of the WA grain.

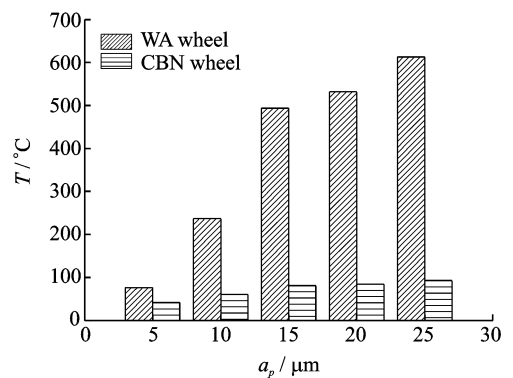


Fig. 8 Comparisons of grinding temperatures

After having been removed 700 mm^3 CSS-42L, the topography of the worn brazed CBN wheel was demonstrated in Fig. 9. It was hard to find any chip adhered to the wheel surface.

4 Conclusions

(1) Grinding forces required in plunge grinding of CSS-42L with the WA wheel were more than that of C45 steel. The highest normal grinding force and tangential force were 115 N and

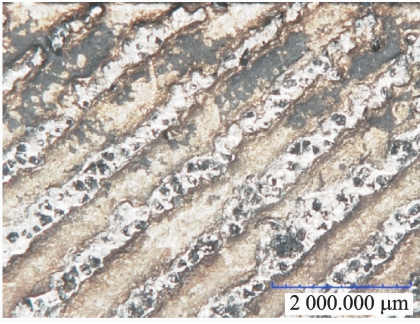


Fig. 9 Topography of worn brazed CBN wheel

53 N, which was about 2.5 times and twice as much as those of C45 steel, respectively.

(2) Chips of CSS-42L adhered to the wheel surface and the adhesion area was about 20% of the whole wheel surface after removing 375 mm³ workpiece materials. At the same time, little adhesion was found after 800 mm³ workpiece of C45 steel were removed.

(3) Grinding forces and temperatures of CSS-42L reduced obviously by using the brazed CBN wheel, and the maximum decreasing amplitude of grinding force was about 70% and that of temperature was about 80%.

Acknowledgements

This work was supported in part by the National Natural Science Foundation of China (Nos. 51305200, 51235004) and the Natural Science Foundation of Jiangsu Province (No. BK20130805).

References:

[1] HANDSCHUH R, KILMAIN D, EHINGER R, et al. Gear design effects on the performance of high speed helical gear trains as used in aerospace drive systems[C] // American Helicopter Society 69th Annual Forum. Phoenix, USA: American Helicopter Society International, 2013: 1791-1798.

[2] ZHAO Z Y. Development of higher-performance aeronautical gear steel[J]. *Journal of Aeronautical Materials*, 2000, 20(3): 148-157. (in Chinese)

[3] SHANIAVSKI A A, SKVORTSOV G V. Crack growth in the gigacycle fatigue regime for helicopter gears[J]. *Fatigue and Fracture of Engineering Materials and Structures*, 1999, 22(7): 609-619.

[4] YILDIRIM N, GASPARINI G, SARTORI S. An improvement on helicopter transmission performance through use of high contact ratio spur gears with

suitable profile modification design[J]. *Proceedings of the Institution of Mechanical Engineers, Part G: Journal of Aerospace Engineering*, 2008, 222(8): 1193-1210.

[5] DEMPSY P J, LEWICKI D G, LE D D. Investigation of current methods to identify helicopter gear health[C] // *Aerospace Conference*. Alexandria: IEEE, 2007: 1-13.

[6] LI H W, ZHANG B L, CHEN L. Interview of academician Zhao Zhen-ye[J]. *Aeroengine*, 2009, 35(3): 1-4. (in Chinese)

[7] ERWIN V Z. Bearing and gear steels for aerospace applications: NASA Technical Memorandum, 102529[R]. 2000.

[8] BOGDAN W K, RYSZARD W. Residual stress in grinding[J]. *Journal of Materials Processing Technology*, 2001, 109(3): 254-257.

[9] DING W F, XU J H, CHEN Z Z, et al. Grindability and surface integrity of cast nickel-based superalloy in creep feed grinding with brazed CBN abrasive wheels[J]. *Chinese Journal of Aeronautics*, 2010, 23(4): 504-509.

[10] KARPUSCHEWSKI B, KNOCHÉ H J, HIPKE M. Gear finishing by abrasive processes[J]. *CIRP Annals-Manufacturing Technology*, 2008, 57(2): 621-640.

[11] Editorial Committee. *China aeronautical materials handbook*[M]. Beijing: Standards Press of China, 2002. (in Chinese)

[12] MURTHY J K N, CHATTOPADHYAY A B, CHAKRABARTI A K. Studies on the grindability of some alloy steels[J]. *Journal of Materials Processing Technology*, 2000, 104(1/2): 59-66.

[13] TSO P L. Study on the grinding of Inconel 718[J]. *Journal of Materials Processing Technology*, 1995, 55(3/4): 421-426.

[14] AMAMOU R, BEN F N, FNAIECH F. Improved method for grinding force prediction based on neural network[J]. *International Journal of Advanced Manufacturing Technology*, 2008, 39(7/8): 656-668.

[15] LIU Q, CHEN X, WANG Y, et al. Empirical modelling of grinding force based on multivariate analysis [J]. *Journal of Materials Processing Technology*, 2008, 203(1/2/3): 420-430.

[16] TSO P L, WU S H. Analysis of grinding quantities through chip sizes[J]. *Journal of Materials Processing Technology*, 1999, 95(1/2/3): 1-7.

[17] MALKIN S, GUO C S. Grinding technology theory and applications of machining with abrasives[M].

New York: Industrial Press, 2008.

- [18] DING W F, XU J H, CHEN Z Z, et al. Wear behavior and mechanism of single-layer brazed CBN abrasive wheels during creep-feed grinding cast nickel-based superalloy[J]. International Journal of Advanced Manufacturing Technology, 2010, 51 (5): 541-550.
- [19] YANG C Y, XU J H, DING W F, et al. Dimension accuracy and surface integrity of creep feed ground titanium alloy with monolayer brazed CBN shaped wheels[J]. Chinese Journal of Aeronautics, 2010, 23 (5): 585-590.
- [20] CHEN Y, DING L Y, FU Y C, et al. Dry grinding of titanium alloy using brazed monolayer cbn wheels coated with graphite lubricant[J]. Transactions of Nanjing University of Aeronautics and Astronautics, 2014, 31(1): 104-109.
- [21] TEICHER U, KUNANZ K, GHOSH A. Performance of diamond and CBN single-layered grinding wheels in grinding titanium[J]. Materials and Manufacturing Processes, 2008, 23(3): 224-227.
- [22] MIAO Q, DING W F, ZHU Y J, et al. Joining interface and compressive strength of brazed cubic boron nitride grains with Ag-Cu-Ti/TiX composite fillers[J]. Ceramics International, 2016, 42 (12): 13723-13737.
- [23] FU Y C, ZHANG Z W, XU J H, et al. High efficiency deep grinding of directional solidified nickel-based superalloy turbine blade root[J]. Journal of Nanjing University of Aeronautics & Astronautics,

2014, 46(2): 190-196. (in Chinese)

Dr. **Yang Changyong** received the B. S. and Master degrees in material science and engineering from Southeast University, Nanjing, in 2002 and Ph. D. degree in mechanical manufacturing and automation from Nanjing University of Aeronautics & Astronautics (NUAA), Nanjing, China, in 2011. He joined in NUAA in May 2011, where he is an associate professor of the College of Mechanical and Electrical Engineering. His research is focused on high efficiency machining of difficult-to-cut materials and relevant fields.

Prof. **Xu Jihua** is a professor of the College of Mechanical and Electrical Engineering, Nanjing University of Aeronautics & Astronautics. His research is focused on high efficiency precision machining of difficult-to-cut materials and relevant fields.

Prof. **Fu Yucan** is a professor of the College of Mechanical and Electrical Engineering, Nanjing University of Aeronautics & Astronautics. His research is focused on high efficiency precision machining of difficult-to-cut materials and relevant fields.

Prof. **Ding Wenfeng** is a professor of the College of Mechanical and Electrical Engineering, Nanjing University of Aeronautics & Astronautics. His research is focused on manufacturing technology of brazed CBN grinding tools and high efficiency grinding.

Prof. **Su Honghua** is a professor of the College of Mechanical and Electrical Engineering, Nanjing University of Aeronautics & Astronautics. His research is focused on high efficiency precision machining of difficult-to-cut materials and relevant fields.

(Executive Editor: Zhang Bei)

